Classification: Biological Science, Neuroscience

Dissociation of *Per1* and *Bmal1* circadian rhythms in the suprachiasmatic nucleus in parallel with behavioral outputs

Daisuke Ono*[1], Sato Honma*[2], Yoshihiro Nakajima[3], Shigeru Kuroda[4], Ryosuke Enoki[1,2,5], and Ken-ichi Honma[2]

[1]Photonic Bioimaging Section, Research Center for Cooperative Projects, Hokkaido University Graduate School of Medicine, Sapporo, 060-8638, Japan
[2]Department of Chronomedicine, Hokkaido University Graduate School of Medicine, Sapporo, 060-8638, Japan
[3]Health Research Institute, National Institute of Advanced Industrial Science and Technology (AIST), Takamatsu, Kagawa 761-0395, Japan
[4]Research Institute for Electronic Science, Hokkaido University, Sapporo, 001-0020, Japan
[5]Precursory Research for Embryonic Science and Technology (PRESTO), Japan Science and Technology Agency (JST), Saitama 332-0012, Japan

Corresponding authors*:
Daisuke Ono (dai-ono@riem.nagoya-u.ac.jp)
Phone: +81-52-789-3863
Full address: Furo-cho, Chikusa-ku, Nagoya 464-8601, Japan
Sato Honma (sathonma@med.hokudai.ac.jp)
Phone: +81-11-706-4737
Full address: North 15, West 7, Kita-ku, Sapporo, 060-8638, Japan

Current address of D.O.: Department of Neuroscience II, Research Institute of Environmental Medicine, Nagoya University, Furo-cho, Chikusa-ku, Nagoya 464-8601, Japan

Author contributions
D.O., S.H. K.H. designed the study. D.O. performed experiments. D.O and Y.N. constructed a method of simultaneous measurement of bioluminescence. D.O S.H. and R.E. constructed a method of fluorescence imaging. S.K. made an analytical program for imaging. D.O., S.H. K.H. analyzed data and wrote the

paper.

Short title:
Two dissociable molecular oscillations in the SCN

Key words: clock gene, *in vivo* recording, suprachiasmatic nucleus, photic phase resetting, E and M oscillators

Abstract

The temporal order of physiology and behavior in mammals is primarily regulated by the circadian pacemaker located in the hypothalamic suprachiasmatic nucleus (SCN). Taking advantage of bioluminescence reporters, we monitored the circadian expression rhythms of clock gene *Per1* and *Bmal1* in the SCN of freely moving mice and found that the rate of phase-shifts induced by a single light pulse was different in the two rhythms. The *Per1-luc* rhythm was phase-delayed instantaneously by the light given at the subjective evening in parallel with the activity-onset of behavior rhythm, whereas the *Bmal1-ELuc* rhythm was phase-delayed gradually similar to the activity-offset. The dissociation was confirmed in cultured SCN slices of mice carrying both *Per1-luc* and *Bmal1-ELuc* reporters. The two rhythms in a single SCN slice showed significantly different periods in a long-term culture (3 weeks) and were internally desynchronized. Regional specificity in the SCN was not detected for the period of *Per1-luc* and *Bmal1-ELuc* rhythms. Furthermore, each of them is not synchronized either with circadian intracellular Ca^{++} rhythms monitored by a calcium indicator, GCaMP6s, nor with firing rhythms monitored on a multi-electrodes array dish, although the coupling between the circadian firing and Ca^{++} rhythms persisted during culture. These findings indicate that the

expressions of two key clock genes, *Per1* and *Bmal1*, in the SCN are regulated in such that they may adopt different phases and free-running periods relative to each other and are associated respectively with the expression of activity-onset and -offset.

Significance statement

The circadian clock in the suprachiasmatic nucleus (SCN) regulates the seasonality in physiology and behavior, which is the best characterized by the change in the activity time of behavior rhythm. In nocturnal rodents, the activity time was shortened in long summer days and lengthened in short winter days due to the change in phase-relationship of activity-onset and offset, for which different circadian oscillators are predicted. Taking advantage of *in vivo* monitoring of clock gene expression in freely moving mice, we demonstrated for the first time that the circadian rhythms of *Per1* and *Bmal1* in the SCN are associated differentially with the phase-shifts of activity-onset and -offset, respectively, suggesting the existence of two oscillations with different molecular mechanisms.

/Body

Introduction

In mammals, the circadian pacemaker in the hypothalamic suprachiasmatic nucleus (SCN) entrains to a light-dark cycle and regulates circadian rhythms of behavior and physiology (1, 2). The circadian oscillation in the SCN is autonomous, where clock genes *Per1*, *Per2*, *Cry1*, *Cry2, Clock* and *Bmal1* play crucial roles (3). A heterodimer of *Clock* and *Bmal1* proteins (CLOCK/BMAL1) activates the transcription of *Per* and *Cry* genes, the protein products of which in turn suppress own transactivation by CLOCK/BMAL1, closing a feedback loop. One turn of the auto-feedback loop (core loop) takes approximately 24 hr. On the other hand, *Bmal1* expression is enhanced by RAR-related orphan nuclear receptor (ROR) and repressed by an orphan nuclear receptor RevErb family (α, β) through RORE (4, 5). The expressions of ROR and RevErb family are in turn enhanced by a BMAL1/CLOCK heterodimer via upstream E-box. Thus, the circadian *Bmal1* rhythm is auto-regulated by a feedback loop (*Bmal1* loop) which interlocked with the core loop keeping an antiphasic phase-relationship with *Per1* rhythm. This interlocked *Bmal1* loop has

been considered to contribute to stabilization and fine tuning of the core loop (4, 6) in addition to the regulation of downstream pathways (7).

The expressions of *Per* genes in the SCN are activated by a timed exposure to light, which phase-shifts the circadian pacemaker (8, 9). The phase-dependent phase shifts of clock gene expression are regarded as a key mechanism of entrainment of the circadian pacemaker to a light-dark cycle. Light signals from the retina stimulate the expressions of *Per* genes, perturbing the core loop dynamics to produce a phase-dependent phase-shift (8). However, the mechanisms of transduction of light-induced phase-shift signals from the core loop to the circadian rhythms in physiology and behavior are not well understood.

On behavior level, the onset and offset of an activity band (activity-onset and -offset) of circadian behavior rhythm are known to differentially respond to a phase-shifted light-dark cycle (10) and to a single light pulse under continuous darkness (DD) in nocturnal rodents (11). In addition, the phase-relation between the activity-onset and -offset is known to change under different photoperiods (12). Furthermore, the two phases of behavior rhythm occasionally split under constant light condition (12). From these findings, the

two oscillator hypothesis was advanced for circadian behavior rhythm in nocturnal rodents (13). Namely, one oscillator designated as an evening (E) oscillator regulates the activity-onset and the other oscillator designated as a morning (M) oscillator controls the activity-offset. Previously, regional differences were reported in the circadian rhythms of clock gene expression in the SCN (14-17), and the phase-relation of the two rhythms was changed under different photoperiods in parallel with the change in activity time of circadian behavior rhythm. These findings suggested an existence of the E and M oscillators in the SCN. However, the molecular mechanism underlying the E and M oscillators are totally unknown. Recently, we developed an *in vivo* method for monitoring the clock gene expression in the SCN of a freely moving mouse (18, 19), which enabled us to compare the SCN circadian rhythms with rhythms in physiology and behavior.

In the present study, in order to obtain an insight into the molecular mechanism of light entrainment, we continuously monitored circadian rhythms in clock gene *Per1* and *Bmal1* expression in the SCN together with behavior rhythms. Surprisingly, the *Per1* and *Bmal1* expression rhythms differentially responded to the light pulse. The dissociation between the two circadian

rhythms was confirmed in the cultured SCN slice of double transgenic mice carrying luciferase reporters for *Per1* and *Bmal1* expression. These findings indicate that there are at least two circadian pacemakers in the SCN, which have different molecular mechanisms and differentially regulate behavioral outputs.

Results

Differential responses of circadian Per1-luc and Bmal1-ELuc rhythms in the SCN in vivo

We continuously measured clock gene *Per1* and *Bmal1* expression in the SCN of freely moving transgenic mice carrying a bioluminescence reporter (*Per1-luc* or *Bmal1-ELuc*) under constant darkness (DD). Spontaneous locomotor activity was simultaneously monitored by an infrared thermal sensor. Bioluminescence emitted from the SCN was collected with an implanted plastic optical fiber which was connected to a cooled photomultiplier tube (PMT) as described previously (18, 19).

Phase responses of the circadian *Per1-luc* and *Bmal1-ELuc* rhythms in the SCN were examined when a single light pulse of 9 h duration was given at circadian time (CT) 11.5 to make the largest phase-delay shift according to the

previous study (20), where the activity-onset of circadian behavior rhythm was defined as CT12 (Fig. 1, Fig. S1A). We also examined the effect of a light pulse of the same duration given at CT21.5 where phase-advance shifts were expected (Fig. 2, Fig. S1B). Data of the *in vivo* experiments before a phase-delaying light pulse (n = 4 for *Per1* and n = 4 for *Bmal1*) were used in a previous study (18) for calculation of free-running period and estimation of the circadian as well as ultradian phases of behavioral and clock gene expression rhythm.

In response to a light pulse at CT11.5, the activity-onset of the behavior rhythm was immediately phase-delayed by 4.0 ± 0.4 h in *Per1-luc* mice (mean ± SD, n = 4) and by 3.5 ± 0.7 h in *Bmal1-ELuc* mice (n = 4) on average. In contrast, the activity offset was gradually phase-delayed over 4 - 5 cycles by 4.4 ± 0.3 h in *Per1-luc* mice and 3.6 ± 0.8 h in *Bmal1-ELuc* mice before reaching a steady state free-running (Fig. 1C-D). The amounts of phase-shifts were not significantly different in either behavioral marker between the two reporter mice. Thus, the activity band was temporarily compressed after the light pulse (Fig. 1C). On the other hand, the circadian peak of *Per1-luc* rhythm was immediately phase-delayed in parallel with the activity-onset (Fig. 1C left and 1D), and that of

Bmal1-ELuc rhythm was gradually phase-delayed in parallel with the activity-offset (Fig. 1C right and 1D). The amount of phase-shift on the second day after the light pulse was significantly different between the two bioluminescent rhythms (two-way ANOVA, post-hoc t-test, $P < 0.05$) (Fig. 1D left). When compared each bioluminescent rhythm with behavior rhythms, the amount of phase-shift in the *Per1-luc* rhythm was not different from that of activity-onset, but significantly different from the activity-offset (Fig. 1D middle) (two-way ANOVA, post-hoc t-test, $P < 0.05$). The amount of phase-shift in the *Bmal1-ELuc* rhythm was not different from that of activity-offset, but significantly different from the activity-onset (Fig. 1D right) (two-way ANOVA, post-hoc t-test, $P < 0.01$).

When a single light pulse was given at CT21.5, the amount of phase-shifts was small and the dissociation was not detected at statistically significant levels between the circadian *Per1-luc* and *Bmal1-ELuc* rhythm (Fig. 2 and Fig. S1B). Nevertheless, a similar association of the circadian peak was observed in clock gene expression with the behavior marker to those observed by a light pulse at CT11.5. These results indicate that the circadian *Per1* and *Bmal1* expression rhythms are dissociable when external perturbation produces

a large phase-delay shift in the SCN circadian rhythm *in vivo*.

Dissociation of Per1 and Bmal1 oscillations in the SCN slice

To test whether the dissociation of circadian *Per1* and *Bmal1* oscillation really occurs, we made SCN slices from the double transgenic mice carrying both reporters for *Per1* and *Bmal1* expression and monitored *Per1-luc* and *Bmal1-ELuc* simultaneously from the same SCN slice. Circadian *Per1-luc* and *Bmal1-ELuc* rhythms in the cultured SCN were successfully separated as previously reported (21, 22) and persisted at least for 3 weeks (Fig. S2).

In the neonatal SCN (Fig. 3A-C), double-plotted circadian rhythms in *Per1-luc* and *Bmal1-Eluc* showed internal dissociation with a pattern similar to relative coordination in which the phase-relation of two rhythms continuously changed in the course of free-running (23). Similar patterns were also detected in other neonatal SCN slices (Fig. S3A). The mean circadian period of *Bmal1-ELuc* mice was significantly shorter than that of *Per1-luc*. Circadian period determined by χ square periodogram was 22.7 ± 0.4 h for *Bmal1-ELuc* and 23.1 ± 0.4 h for *Per1-luc,* which were significantly different (n = 9, pared t-test, $P < 0.01$) (Fig. 3D). The periods determined by other methods such as a

liner regression line fitted to the consecutive cycle peaks confirmed the difference (Fig. S3B). As a result, the phase-relation between the circadian *Per1-luc* and *Bmal1-ELuc* rhythms was gradually and significantly changed during culturing (Fig. 3C, Fig. S3A), regardless of the circadian phase-marker used: the acrophase of a fitted cosine curve (Fig. 3I, Fig. S3C left) or the peak of a detrended circadian rhythm (Fig. S3C right). To know whether or not the changes of the phase-relationship between the two circadian rhythms reflected gradual and systematic alterations of the rhythm shape, we compared the shape of rhythmicity on day 3 and day 15 of culture and did not find any difference (Fig. S3D). In addition, the skewness of circadian rhythm was not significantly different between day 3 and day 15 for both *Per1-luc* and *Bmal1-ELuc*. Furthermore, to exclude a possible effect of rhythm damping during culture on the determination of rhythm phase, we enhanced the rhythm amplitude by replacing culture medium with fresh one, which is known to increase the robustness of rhythmicity (Fig. S4). However, since the medium exchange is also known to shift the circadian rhythm of the neonatal SCN depending on the time of replacement (24), we selected the time in order to minimize the phase-shifts. The phase relation between the two rhythms was essentially kept

as it had been after medium exchange and there was no systematic relation between the rhythm amplitude and phase-difference.

A difference in the circadian period between the two clock gene rhythms was also detected in the adult SCN slice (Fig. 3E-H, Fig. S3). The circadian period of *Per1-luc* rhythm was 23.4 ± 0.1 h and that of *Bmal1-ELuc* rhythm was 23.2 ± 0.1 h (n = 5), which was significantly different (Fig. 3H, paired t test, $P < 0.01$). However, the amount of dissociation in the adult SCN was less robust and the phase-difference between the two rhythms after the 11th culture day was significantly smaller in the adult than in the neonatal SCN (Fig. 3I) ($P < 0.01$, two-way repeated measure ANOVA).

Spontaneous firing rhythms in the cultured SCN is dissociated from Per1 and Bmal1 oscillations

Spontaneous firing is regarded as an important output signal from a core loop in the SCN (25, 26) and well correlated with circadian behavior rhythms (27). However, the mechanism remains unknown how spontaneous firings in the SCN regulate circadian behavioral rhythms. To understand the relationship between the circadian firing rhythm and the activity onset or offset, or between

spontaneous firing and clock gene expression in the SCN, we measured *Per1-luc* or *Bmal1-ELuc* simultaneously with spontaneous firing in the neonatal SCN slices using a multi-electrode array dish (MED) and CCD camera (Fig. 4A and B, Fig. S6A and B). For this experiment, we used single transgenic mice carrying a bioluminescence reporter for *Per1-luc* or *Bmal1-ELuc* expression. These single transgenic mice showed similar characteristics of the circadian bioluminescent rhythms to those of double transgenic mice (*Per1-luc*, 23.3 ± 0.1 h, n = 7; *Bmal1-ELuc*, 22.7 ± 0.3 h, n = 7, student's t-test, $P < 0.01$) (Fig. S5).

The circadian peak of *Per1-luc* rhythm in the neonatal SCN slice on the MED was gradually phase-delayed relatively to that of the spontaneous firing rhythms (Fig. 4C-E). On the other hand, the circadian peak of *Bmal1-ELuc* rhythm was gradually phase-advanced relatively to that of the firing rhythms (Fig. 4C-E). The phase difference between the firing rhythms and *Per1* or *Bmal1* expression rhythms was significantly larger at the 15th culture day than that at the beginning of culture (Fig. 4F) (Student's t-test, $P < 0.01$). Circadian periods of *Per1-luc* and *Bmal1-ELuc* rhythms were also significantly different (Fig. 4G) (Student's t-test, $P < 0.05$). These results indicate that the firing rhythms and *Per1* or *Bmal1* rhythms in the cultured SCN are dissociable and that the firing

rhythms are not a direct consequence of circadian oscillation either of the core feedback loop or of the interlocked *Bmal1* loop.

Spatiotemporal features of Per1 and Bmal1 expressions in the cultured SCN

In order to know whether or not the dissociation between the circadian *Per1* and *Bmal1* rhythms is due to the region specific gene expression in the SCN, we analyzed the spatiotemporal feature of *Per1-luc* and *Bmal1-ELuc* expressions in the SCN during culturing using an automated rhythm analysis with time-series images on the pixel level (28). In both *Per1-luc* and *Bmal1-ELuc* rhythms, the mean circadian phase on the 2-3 culture day was significantly delayed in the ventral region relative to the dorsal by ca. 1 hour for *Per1-luc* (paired t-test, $P < 0.05$) and by ca. 3 hours for *Bmal1-ELuc* (paired t-test, $P < 0.05$) (Fig. 4J and L). The phase-relation between the dorsal and ventral regions was not changed on the 13-14 culture days either in the *Per1-luc* or *Bmal1-Eluc* rhythm (paired t-test, *Per1-luc*, $P = 0.841$; *Bmal1-ELuc*, $P = 0.932$ Fig. 4J and L). We also analyzed the circadian peak distributions in the dorsal and ventral regions of the SCN using Rayleigh plot (Fig. 4K and M, Fig. S6C and D). The

mean vector of the circadian rhythm was not changed in the dorsal and ventral regions of the SCN during culturing for both *Per1-luc* (Fig. 4K) and *Bmal1-ELuc* (Fig. 4M), suggesting the internal synchrony of cellular circadian rhythms was kept unchanged during culture. These results indicate that the dissociation between *Per1-luc* and *Bmal1-ELuc* rhythms is not due to a regional difference in the SCN neural network.

Simultaneous measurement of circadian Per1, Bmal1, calcium, and spontaneous firing in the cultured SCN

To further understand relationships among the circadian firing rhythm, the core feedback loop and interlocked *Bmal1* loop, we simultaneously measured *Per1* and *Bmal1* gene expressions, spontaneous firing and intracellular calcium level from single cultured SCN slices. The SCN of double transgenic mice (*Per1-luc* and *Bmal1-ELuc*) expressing GCaMP6s was cultured on an MED probe and monitored bioluminescence of firefly (F)-luc for *Per1-luc* and E-luc for *Bmal1-ELuc*, fluorescence of GCaMP6s, and spontaneous firing (Fig. 5A and B, Fig. S7, Movie S1). In addition to an endogenous circadian oscillation as an output of the core feedback loop, intracellular calcium in the

SCN is known to be controlled by the input signals from the SCN neural network (29, 30). Plotting of acrophase or of circadian peak in each cycle revealed that the circadian rhythms in *Bmal1-ELuc*, spontaneous firing, and intracellular calcium were gradually phase-advanced relative to the circadian *Per1-luc* rhythms in a course of culturing (Fig. 5C-H) (one-way repeated measure ANOVA, $P < 0.05$, post-hoc Tukey-Kramer test). Interestingly, circadian calcium rhythm was essentially phase-locked to the circadian firing rhythms keeping a stable phase difference of about 1 hour for over 10 days (Fig. 5D, 5H). Thus, the phase-relations of circadian *Per1-luc*, *Bmal1-ELuc* and firing rhythms were gradually changed during culturing. Although the phase-relations among these circadian rhythms were substantially changed during culture, the phase-relation of the circadian *Per1-luc* and *Bmal1-ELuc* rhythms (Δphase) was not changed between the dorsal and ventral SCN regions (Day2-3, 1.7 ± 0.3 h; Day13-14, 2.1 ± 0.9 h, pared t-test, $P = 0.283$) (Fig. 5F, G and Fig. S7C), suggesting a change in the phase-relationship of the two rhythms occurred at the same rate in both regions. The mean vector was not different between day 2 - 3 and day 13 -14 in these circadian rhythms suggesting again the internal synchrony of cellular circadian rhythms was kept during culture (Fig. S7D). On the other hand, the

mean vector of the circadian *Bmal1-ELuc* was slightly but significantly shorter than those of the other circadian rhythms, suggesting either differential internal synchrony and/or sloppiness of the circadian *Bmal1-luc* rhythms

Discussion

In the present study, we found that the circadian *Per1-luc* and *Bmal1-ELuc* rhythms were transiently dissociated when a phase-shifting light pulse was given in freely moving mice under DD. The gene expression rhythms were differentially associated with the activity onset and offset of circadian behavior rhythm. Similar dissociation of *Per1* and *Bmal1* oscillation was observed in the cultured SCN slices of mice carrying a dual reporter system. Such a transient dissociation between the circadian rhythms was detected only by continuous and simultaneous measurement of multiple rhythms from a single SCN. The dual reporter system used in the present study enabled us to identify the change in phase relation of two different rhythms for the first time. However, since the method is based on luciferin-luciferase reaction and separation of emitted lights by filtering, these findings should be confirmed by more direct measurement of transcription or translation of clock genes in future. Most of the

current direct methods are still difficult to apply because of insufficient time resolution due to individual difference and usage of a large number of animals.

Interestingly, the circadian rhythm in spontaneous firing was dissociated from the circadian *Per1* and *Bmal1* rhythms but not from the circadian rhythm in intracellular calcium level. These findings indicate that the *Bmal1* loop has an oscillatory nature similar to the core loop and behaves as a constitutional subunit of the circadian system in the SCN.

We demonstrated the dissociation of circadian rhythms in clock gene expression in freely moving mice when the circadian rhythms were in transients of a light-induced phase-delay shifts (Fig. 1). A similar dissociation of circadian clock gene expression rhythms has been observed previously under LD shift schedules (31, 32), but the relevance to behavior outputs was not clear. Importantly, the phase-shifts of *Per1* and *Bmal1* rhythms in our study were closely associated with the phase-shifts of either of the activity-onset or -offset of behavior rhythm. Previously, Vansteensel et al. (33) reported the dissociation between the circadian *Per1-luc* rhythm in the SCN and behavioral rhythms, which occurred following a shift of light-dark cycle. The finding raised the possibility that the circadian *Per1-luc* rhythm reports only a subset of SCN

neurons. In consistent with this report, the present findings suggest not only the existence of two coupled circadian oscillations with different molecular mechanisms but also their differential association with the activity onset and offset of behavior rhythms. According to the Pittendrigh's hypothesis (13), the activity-onset and -offset of nocturnal rodents are regulated by two different oscillators called an evening (E) and morning (M) oscillator, respectively. The hypothesis was based on the findings of rhythm splitting under constant light and differential responses to lights (12). In consistent with the above hypothesis, Honma et al (1985) demonstrated in rats that the activity-onset and the -offset showed different phase-responses to a single light pulse (11). Thus, the circadian *Per1-luc* rhythm in the SCN seems to associate with the E oscillator, whereas the circadian *Bmal1-ELuc* rhythm with the M oscillator. Previous reports demonstrated separate regional pacemakers which behaved differentially under a long and a short photoperiod in the SCN (14, 15). The pacemaker corresponding to the E oscillator is likely located in the rostral part of SCN and that corresponding to the M oscillator in the caudal part. The present findings further suggest that molecular mechanism of two circadian oscillations is different.

Dissociation between the *Per1* and *Bmal1* oscillation was also observed in the SCN in *ex vivo* (Fig. 3-5). Due to a significant difference in the circadian period, the phase-relation between the *Per1* and *Bmal1* oscillation gradually changed during culturing, which was not due to the systematic changes in the shapes of circadian rhythms (Fig. S3 and Fig. S7). The core and interlocked *Bmal1* loop have been regarded as the origin of the circadian *Per1* and *Bmal1* expression rhythms (3-5). The present results indicate that the two loops are coupled to each other, but that they exhibit ongoing differences in period and relative phase that suggest they may oscillate independently. They are dissociable by a light pulse *in vivo* and by prolonged free-run in *ex vivo*. The theoretical backgrounds of the present findings are a coupling of two oscillating feedback loops and a dependency of circadian period on a relative strength of interlocked loops as formulated in another associated loop (34). In addition, relative coordination between of *Per1-luc* and *Bmal1-ELuc* rhythms suggests that the core loop and *Bmal1* loop are not independent but mutually interactive even under dissociation. The *Bmal1* loop consists of a positive feedback component of ROR and a negative feedback component of RevErbα for *Bmal1* expression, which is potentially capable of oscillating without oscillation of the

core loop at least from a theoretical view point (35).

The circadian oscillation in the dorsomedial region of the SCN was reported to be faster than that in the ventrolateral region (36). Regional differences were also reported in the intensity of clock gene expression (37). Therefore, the dissociation between the two clock gene rhythms could be ascribed to the regional differences in the circadian oscillation. However, in the present study, the phase-relation of the *Per1* and *Bmal1* expression rhythms was not different between the dorsal and ventral SCN during culturing, questioning the possibility of regional difference of respective circadian oscillation as a cause of dissociation. Recently, we found sharply differentiated clusters of cells which expressed the circadian PER2 rhythm with different periods in the SCN of *Cry1,2* double deficient mice (38). The cells consisting of each of these cell clusters showed no regional specificity but rather diffusely distributed. The finding suggested that in the SCN circadian system a specific type of oscillating cells builds up a constitutional oscillator that does not necessarily show regional specificity. The *Per1* and *Bmal1* specific oscillator cells could be located diffusely throughout the SCN. Alternatively, the dissociation of two clock gene rhythms could be due to dissociation of the core

loop and *Bmal1* loop in single SCN cells. If so, despite of a single cell, the core molecular loop would be responsible for the activity onset, while the *Bmal1* loop for the activity-offset of behavior rhythm, respectively. In this case, we should assume different output signals from a single cell. In any case, the coupling of two oscillations was less strong in the neonatal SCN than in the adult, suggesting a developmental change in the circadian system in the SCN.

We had expected that the circadian firing rhythm in the SCN slice might synchronize with either of the two clock gene expression rhythms or show a splitting into two components. Contrary to our expectation, the simultaneously determined circadian firing rhythms dissociated from both of the circadian gene expression rhythms (Figs. 4, 5). However, a coupling between the circadian firing and intracellular calcium rhythms persisted at least for 2 weeks in culture, suggesting that the two overt rhythms are regulated by the same oscillatory mechanism which could be neither the core loop nor the interlocked *Bmal1* loop. The cellular circadian rhythms in the SCN are likely regulated by two circadian oscillations of different origins: the intracellular molecular feedback-loop and the SCN network the cell involved in. Relative intensities of the two oscillations may determine the nature of cellular circadian rhythms examined. Circadian firing and

calcium rhythms would be affected by feedback loops and SCN network (39). A strong coherence of the circadian firing rhythm to the intracellular calcium rhythm could be interpreted in terms of causality rather than of oscillatory coupling. Neither Ca^{2+} nor firing rhythm in the SCN is directly associated with onset or offset of circadian behavioral rhythm. The present findings indicate that the links between the SCN circadian rhythms and behavior is more complicated than ever thought (40).

Taken together, the present findings indicate that external perturbation such as a single light pulse transiently uncouples interlocked molecular loops which are separately associated with the onset and offset of behavior rhythms.

Materials and Methods

Animals

Male and female *Per1-luc* (heterozygous or homozygous) (14) and *Bmal1-ELuc* (heterozygous) (41) reporter mice of C57BL/6j background were used. *Per1-luc* and *Bmal1-ELuc* mice were produced in YS New Technology Institute (Tochigi, Japan) and National Institute of Advanced Industrial Science

and Technology (Tsukuba, Japan), respectively, by injecting reporter construct to fertilized eggs of C57BL/6j background. We back-crossed these mice with C57BL/6j background mice as well for more than 7 generations. Mice were reared in our animal quarters where environmental conditions were controlled (lights-on 6:00-18:00; light intensity approximately 100 lux at the cage bottom; humidity 60 ± 10%). Mice had free access to food pellets and water. Experiments were conducted in compliance with the rules and regulations established by the Animal Care and Use Committee of Hokkaido University under the ethical permission of the Animal Research Committee of Hokkaido University (Approval No. 13-0053 for in vivo experiment and No. 13-0064 for ex vivo experiment).

Behavioral activity measurement

Mice were used in the *in vivo* study at 2-6 months old (9 males, 4 females). Mice were individually housed in a polycarbonate cage (115 mm wide, 215 mm long, 300 mm high) which was placed in a light-tight and air-conditioned box (40 x 50 x 50 cm). An LED light source was equipped on the ceiling of a box and turned-on when a light pulse was given 5 days after exposure to DD. The

light intensity was 150-250 lux. Spontaneous movements were measured by a passive infrared sensor which detects a change in thermal radiation from an animal due to body movements (42). The amount of behavior activity was automatically recorded every one minute by a computer (The Chronobiology Kit; Stanford Software System).

Surgery

Surgery was performed according to the method described previously (18, 19). Surgical operation was performed under isoflurane anesthesia. To measure bioluminescence from the SCN *in vivo*, a handmade guide cannula (inner diameter 1.12 mm, outer diameter 1.48 mm) was stereotaxically inserted into the brain (0.2 mm posterior to the bregma and 0.2 mm lateral from the midline, and 3.0 mm from the surface of the skull) and fixed to the skull with dental resin. After a recovery period of more than 4 days, a polymethyl methacrylate optical fiber (fiber diameter, 0.5 mm; surface cladding, 0.25 mm thick) was inserted into the guide cannula aimed at the SCN (5.8 mm depth from the surface of the skull) and fixed to the skull with dental resin.

More than 4 days after the insertion of the optical fiber, an osmotic pump

containing luciferin, a substrate of luciferase, was implanted. To deliver the substrate, the osmotic pump (flow speed, 0.5 μl/h, pump volume; 200μl, 2002, Alzet, Cupertino, California, USA) was filled with D-luciferin K (100 mM) dissolved in physiological saline and implanted in the peritoneal cavity. After each surgery, penicillin-G was used to prevent infection (40 unit/g of body weight, intra-muscular injection). As for post-operative analgesia, we used aspirin (120mg/kg of body weight, per os) or buprenorphine (0.05 - 0.1mg/kg of body weight, subcutaneous injection).

***In vivo* measurement of bioluminescence**

Three to five days after the implantation of an osmotic pump, bioluminescence was measured from the SCN in freely moving mice under DD. The measurement was performed every one minute via an optical fiber connected to a photon counting device (18, 19) (In vivo Kronos, Atto, Tokyo, Japan) equipped with a photomultiplier tube (Hamamatsu Photonics, Hamamatsu, Shizuoka, Japan). Recorded data were fed into a computer and analyzed.

Histological examination

Once the measurements were completed, mice were anesthetized with ether and intracardially perfused with physiological saline, followed by 4% paraformaldehyde in 0.1M phosphate buffer (PB). Brains were cryoprotected with 20 % sucrose in 0.1M PB. Serial coronal sections of the brain with 30 μm thick were made using Cryostat (Leica) and stained with cresyl violet to identify the localization of the tip of the optical fiber.

SCN slice preparation for culture

For the measurement of bioluminescence from the SCN slice, mice were euthanized to harvest the SCN between 8:00 and 16:00 h. For the tissue level measurement, the coronal SCN slices of 300 μm thick were made with a tissue chopper (Mcllwain) from the neonatal mice (postnatal day 7: P7) and with a microslicer (DTK-1000; Dosaka EM) from the adults (2-6 months old). The SCN tissue was dissected at the mid-rostrocaudal region and a paired SCN was cultured on a Millicell-CM culture insert (Millipore Corporation). The culture conditions were the same as those described previously (43). Briefly, the slice was cultured in air at 36.5 ºC with 1.2 ml Dulbecco's modified Eagle's medium

(Invitrogen) with 0.1 mM D-luciferin K and 5 % supplement solution.

Measurement of bioluminescence on the SCN tissue level

Bioluminescence on the SCN tissue level was measured using a PMT (Lumicycle; Actimetrics or Kronos; Atto) at 10 min intervals with an exposure time of 1 min. For the simultaneous measurement of *Per1* and *Bmal1* expression, bioluminescence of *Per1-luc* and *Bmal1-ELuc* from the same SCN slice was monitored alternatively by a dish type luminometer with a turntable for 8 recording dishes (Kronos, Atto). Bioluminescence was measured for each 15 sec in the presence of a 600 nm long-pass filter (R60 filter, Hoya), then a 560 nm long-pass filter (O56 filter, Hoya), and without any filter. The measurement was repeated at 10 min intervals. The intensities of *Per1-luc* and *Bmal1-ELuc* bioluminescence were calculated as described previously (21, 22). For bioluminescence calculation, we used a 600 nm long-pass filter.

Simultaneous recordings of bioluminescence and spontaneous firing from an SCN slice

The SCN slice from a 3 - 5 day old pup was cultured on a Multi-electrode

array dish (MED). The MED with 64 electrodes was used for the SCN slice culture. The size of an electrode was 20 × 20 μm (MED-P210A). Spontaneous firings were recorded using a MED 64 system (Alpha MED Scientific). Spike discharges with a signal-noise ratio >2.0 were collected by Spike Detector software (Alpha MED Scientific) as previously described (43). The number of spikes per min was calculated for each electrode covered by an SCN slice.

The MED was placed in a mini-incubator installed on the stage of a microscope (ECRIPSE TE2000-U, ECRIPSE E1000, Nikon). The culture conditions were the same as those described previously (43). Bioluminescence was recorded with a CCD camera (ORCA-II, Hamamatsu Photonics) cooled at -60 ºC. The pixel size was 4.3 × 4.3 μm.

Simultaneous recordings of *Per1-luc*, *Bmal1-ELuc*, calcium, and spontaneous firing from an SCN slice

The SCN slice from a 3 - 5 day old pup of *Per1-luc* and *Bmal1-ELuc* mice was cultured on a Millicell-CM culture insert. Aliquots of adeno-associated virus (AAV; serotype rh10) harboring GCaMP6s, a genetically encoded calcium sensor under the control of human synapsin-1 promotor (University of

Pennsylvania Gene Therapy Program Vector Core), were inoculated onto the surface of the cultured SCN slice 3 - 5 days after the preparation of the slice. On the next day of AAV infection, the SCN slice was transferred onto the MED probe. Seven to ten days after culturing the SCN, simultaneous measurement of bioluminescence, fluorescence, and neuronal activity was started.

The MED was placed in a mini-incubator installed on the stage of a microscope (ECRIPSE-80i, Nikon) equipped with EM-CCD camera (ImagEM, Hamamatsu photonics). Fluorescent calcium sensor (GCaMP6s) was excited at cyan color (475/28 nm) with LED light source (Retra Light Engine; Lumencor), and visualized with 495 nm dichroic mirror and 520/35 nm emission filters (Semlock). For measuring of F-luc and E-luc bioluminescence (*Per1-luc* and *Bmal1-ELuc*) separately, a long pass filter (AT610) was used. Bioluminescence with or without the filter were measured every 1 hour (exposed time 29 min for each condition). *Per1-luc* and *Bmal1-ELuc* bioluminescence were calculated on the pixel level as the same method of PMT measurement.

Data analysis

For the analyses of behavior rhythms *in vivo*, spontaneous movements

obtained every one minute were used. The amounts of phase-shifts were determined on the basis of a double plotted actograph by visual inspection. A regression line was fitted to the succeeding activity-onsets or -offsets during a steady state free-run before and after the light pulse. The circadian period was determined by the slope of a regression line, and the amount of daily phase shift was calculated from the phase difference between the phase on the day of light pulse and that on the following day. Three experts of chronobiology participated in the visual inspection.

For the analyses of circadian bioluminescent rhythms *in vivo* and *ex vivo*, obtained data with a PMT were smoothed by a four hour moving average method for *in vivo* data and a 50 min moving average for *ex vivo* data, respectively. The smoothed data were then detrended by a 24 hour moving average subtraction method (18, 19). Neuronal activity rhythms were also detrended by a 24 hour moving average subtraction method. For comparing the peak phases of circadian rhythms *in vivo* and *ex vivo*, we used acrophase obtained by ClockLab software (Actimetrics) or simply peak phase in a cycle. Circadian period in the slice SCN was calculated by periodogram or from a slope of a regression line fitted to consecutive peak phases by a least square method.

The phase-angle difference between two circadian rhythms was calculated using, the acrophase of a best fitted cosine curve, or the peak of a circadian cycle. For time-laps images obtained by a CCD camera, the properties of circadian rhythm in bioluminescence and fluorescence signals were analyzed on pixel-level using a custom-made software based on cosine curve fitting method as described previously (39, 44). The dorsal and ventral areas of the SCN were separated by a line drawn at the midpoint between dorsal and ventral edge so that it crosses the third ventricle at a right angle. Rayleigh plot was made using the Oriana4 software (Kovach Computing Service). Data were expressed as mean ± SD unless otherwise indicated as mean ± SEM.

Statistics

Student's t-test was used when two independent group means were compared. Pared t-test was used when two dependent group means were compared. A one-way ANOVA with a post-hoc Tukey-Kramer test was used to analyze a single time series data. A two-way ANOVA with post-hoc t-test was adopted when two independent time series data were compared (Statview or Statcel 3)

Acknowledgements

We thank H. Tei for giving *Per1-luciferase* reporter plasmid. We also thank M. Shimogawara and H. Kubota for the development of an *in vivo* bioluminescence measurement system, K. Baba for technical advice, T. Ueda for analysis program, M. Mieda for advice of AAV purification, and M.P. Butler for thorough discussion. We thank Genetically-Encoded Neuronal Indicator and Effector (GENIE) Project and the Janelia Farm Research Campus of the Howard Hughes Medical Institute for sharing GCaMP6s constructs. This work was supported in part by The Uehara Memorial Foundation, The Nakajima Foundation, the Project for Developing Innovation Systems of the MEXT, and Creation of Innovation Centers for Advanced Interdisciplinary Research Areas Program, Ministry of Education, Culture, Sports, Science and Technology, Japan and JSPS KAKENHI (No. 15H04679, No. 26860156, No. 15K12763).

Competing financial interest

The authors have no competing financial interests.

Reference

1. Moore, R.Y. and Eichler, V.B. (1972) Loss of a circadian adrenal corticosterone rhythm following suprachiasmatic lesions in the rat. *Brain Res.* 42(1): 201-206.
2. Stephan, F.K. and Zucker, I. (1972) Circadian rhythms in drinking behavior and locomotor activity of rats are eliminated by hypothalamic lesions. *Proc. Natl. Acad. Sci. U.S.A.* 69(6): 1583-1586.
3. Reppert, S.M. and Weaver, D.R. (2002) Coordination of circadian timing in mammals. *Nature* 418(6901): 935-941.
4. Preitner, N. et al. (2002) The orphan nuclear receptor REV-ERBalpha controls circadian transcription within the positive limb of the mammalian circadian oscillator. *Cell* 110(2): 251-260.
5. Triqueneaux, G. et al. (2004) The orphan receptor Rev-erbalpha gene is a target of the circadian clock pacemaker. *J. Mol. Endocrinol.* 33(3): 585-608.
6. Sato, T.K. et al. (2004) A functional genomics strategy reveals Rora as a component of the mammalian circadian clock. *Neuron* 43(4): 527-537.
7. Liu, A.C. et al. (2008) Redundant function of REV-ERBalpha and beta and non-essential role for Bmal1 cycling in transcriptional regulation of

intracellular circadian rhythms. *PLoS Genet.* 4(2): e1000023.

8. Shigeyoshi, Y. et al. (1997) Light-induced resetting of a mammalian circadian clock is associated with rapid induction of the mPer1 transcript. *Cell* 91(7): 1043-1053.
9. Albrecht, U., Sun, Z.S., Eichele, G., and Lee, C.C. (1997) A differential response of two putative mammalian circadian regulators, mper1 and mper2, to light. *Cell* 91(7): 1055-1064.
10. Aschoff, J., Hoffmann, K., Pohl, H., and Wever, R. (1975) Re-entrainment of circadian rhythms after phase-shifts of the Zeitgeber. *Chronobiologia* 2(1): 23-78.
11. Honma, K., Honma, S., and Hiroshige, T. (1985) Response curve, free-running period, and activity time in circadian locomotor rhythm of rats. *Jpn. J. Physiol.* 35(4): 643-658.
12. Pittendrigh, C.S. and Daan, S. (1976) A functional analysis of circadian pacemakers in nocturnal rodents. V. Pacemaker structure: A clock for all seasons. *J. Comp. Physiol. A* 106: 333-355.
13. Pittendrigh, C.S. (1974) Circadian oscillation in cells and the circadian organization of multi-cellular systems. In: The Neurosciences, Third Study

Program, Schmitt F.O., Worden F.G., editors. Cambridge: The MIT Press, 437-458.

14. Inagaki, N., Honma, S., Ono, D., Tanahashi, Y. and Honma K. (2007) Separate oscillating cell groups in mouse suprachiasmatic nucleus couple photoperiodically to the onset and end of daily activity. *Proc. Natl. Acad. Sci. U.S.A.* 104(18): 7664-7669.
15. Naito, E., Watanabe, T., Tei, H., Yoshimura, T., and Ebihara, S. (2008) Reorganization of the suprachiasmatic nucleus coding for day length. *J. Biol. Rhythms* 23(2): 140-149.
16. Evans, J.A., Leise, T.L., Castanon-Cervantes, O., and Davidson, A.J. (2013) Dynamic interactions mediated by nonredundant signaling mechanisms couple circadian clock neurons. *Neuron* 80(4): 973-983.
17. Myung, J. et al. (2015) GABA-mediated repulsive coupling between circadian clock neurons in the SCN encodes seasonal time. *Proc. Natl. Acad. Sci. U.S.A.* 112(29): E3920-3929.
18. Ono, D., Honma, K., and Honma, S. (2015) Circadian and ultradian rhythms of clock gene expression in the suprachiasmatic nucleus of freely moving mice. *Sci. Rep.* 5:12310.

19. Ono, D., Honma, S., and Honma, K. (2015) Circadian PER2::LUC rhythms in the olfactory bulb of freely moving mice depend on the suprachiasmatic nucleus but not on behaviour rhythms. *Eur. J. Neurosci.* 42(12): 3128-3137.

20. Comas, M., Beersma D.G., Spoelstra, K., and Daan, S. (2006) Phase and period responses of the circadian system of mice (Mus musculus) to light stimuli of different duration. *J. Biol. Rhythms* 21(5): 362-372.

21. Noguchi, T., Ikeda, M., Ohmiya, Y., and Nakajima, Y. (2008) Simultaneous monitoring of independent gene expression patterns in two types of cocultured fibroblasts with different color-emitting luciferases. *BMC Biotechnol.* 8(40).

22. Noguchi, T., et al. (2010) Dual-color luciferase mouse directly demonstrates coupled expression of two clock genes. *Biochemistry* 49(37): 8053-8061.

23. Aschoff J. (1981) Freerunning and Entrained Circadian Rhythms. *Handbook of Behavioral Neurobiology*, Biological Rhythms, (ed) Jűrgen Aschoff, Plenum Press, New York, pp.81-93.

24. Nishide S.Y., Honma S., and Honma K. (2008) The circadian pacemaker in the cultured suprachiasmatic nucleus from pup mice is highly sensitive to external perturbation. *Eur. J. Neurosci.* 27(10): 2686-90.

25. Schwartz, W.J., Gross, R.A., and Morton, M.T. (1987) The suprachiasmatic nuclei contain a tetrodotoxin-resistant circadian pacemaker. *Proc. Natl. Acad. Sci. U.S.A.* 84(6): 1694-1698.

26. Jones, J.R., Tackenberg, M.C., and McMahon, D.G. (2015) Manipulating circadian clock neuron firing rate resets molecular circadian rhythms and behavior. *Nat. Neurosci.* 18(3): 373-375.

27. Nakamura, W. et al. (2008) In vivo monitoring of circadian timing in freely moving mice. *Curr. Biol.* 18(5): 381-385.

28. Yoshikawa, T. et al. (2015) Spatiotemporal profiles of arginine vasopressin transcription in cultured suprachiasmatic nucleus. *Eur. J. Neurosci.* 42(9): 2678-2689.

29. Ikeda, M. et al. (2003) Circadian dynamics of cytosolic and nuclear Ca2+ in single suprachiasmatic nucleus neurons. *Neuron* 38(2): 253-263.

30. Hastings, M.H., Maywood,E.S., and O'Neill, J.S. (2008) Cellular circadian pacemaking and the role of cytosolic rhythms. *Curr. Biol.* 18(17): R805-815.

31. Reddy, A.B., Field, M.D., Maywood, E.S., and Hastings, M.H. (2002) Differential resynchronisation of circadian clock gene expression within the suprachiasmatic nuclei of mice subjected to experimental jet lag. *J. Neurosci.*

22(17): 7326-7330.

32. Kiessling, S., Eichele, G., and Oster, H. (2010) Adrenal glucocorticoids have a key role in circadian resynchronization in a mouse model of jet lag. *J. Clin. Invest.* 120(7): 2600-2609.

33. Vansteensel, M.J. et al. (2003) Dissociation between circadian Per1 and neuronal and behavioral rhythms following a shifted environmental cycle. *Curr. Biol.* 13(17): 1538-1542.

34. Yan, J. et al. (2014) An intensity ratio of interlocking loops determines circadian period length. *Nucleic Acids Res.* 42(16): 10278-10287.

35. Uryu K. and Tei H. (2016) Feedback loops interlocked at competitive binding sites amplify mammalian circadian oscillations. *J. Chronobiol*. 22(2): 155.

36. Koinuma, S. et al. (2013) Regional circadian period difference in the suprachiasmatic nucleus of the mammalian circadian center. *Eur. J. Neurosci.* 38(6): 2832-2841.

37. Evans, J.A. et al. (2015) Shell neurons of the master circadian clock coordinate the phase of tissue clocks throughout the brain and body. *BMC Biol.* 13(43).

38. Ono, D., Honma, S., and Honma, K. (2016) Differential roles of AVP and VIP

signaling in the postnatal changes of neural networks for coherent circadian rhythms in the SCN. *Sci. Adv.* 2(9): e1600960.

39. Enoki, R. et al. (2012) Topological specificity and hierarchical network of the circadian calcium rhythm in the suprachiasmatic nucleus. *Proc. Natl. Acad. Sci. U. S. A.* 109(52): 21498–503.

40. Ramkisoensing, A., and Meijer, J.H. (2015) Synchronization of Biological Clock Neurons by Light and Peripheral Feedback Systems Promotes Circadian Rhythms and Health. *Front Neurol.* 6(128).

41. Noguchi, T., Ikeda, M., Ohmiya, Y., and Nakajima, Y. (2012) A dual-color luciferase assay system reveals circadian resetting of cultured fibroblasts by co-cultured adrenal glands. *PLOS ONE* 7(5).

42. Abe, H. et al. (2001) Clock gene expressions in the suprachiasmatic nucleus and other areas of the brain during rhythm splitting in CS mice. *Brain Res. Mol. Brain Res.* 87(1), 92-99.

43. Ono, D., Honma, S. and Honma, K. (2013) Cryptochromes are critical for the development of coherent circadian rhythms in the mouse suprachiasmatic nucleus. *Nat. Communs.* 4(1666).

44. Mieda, M. et al. (2015) Cellular clocks in AVP neurons of the SCN are critical

for interneuronal coupling regulating circadian behavior rhythm. *Neuron* 85(5): 1103-1116.

Figures

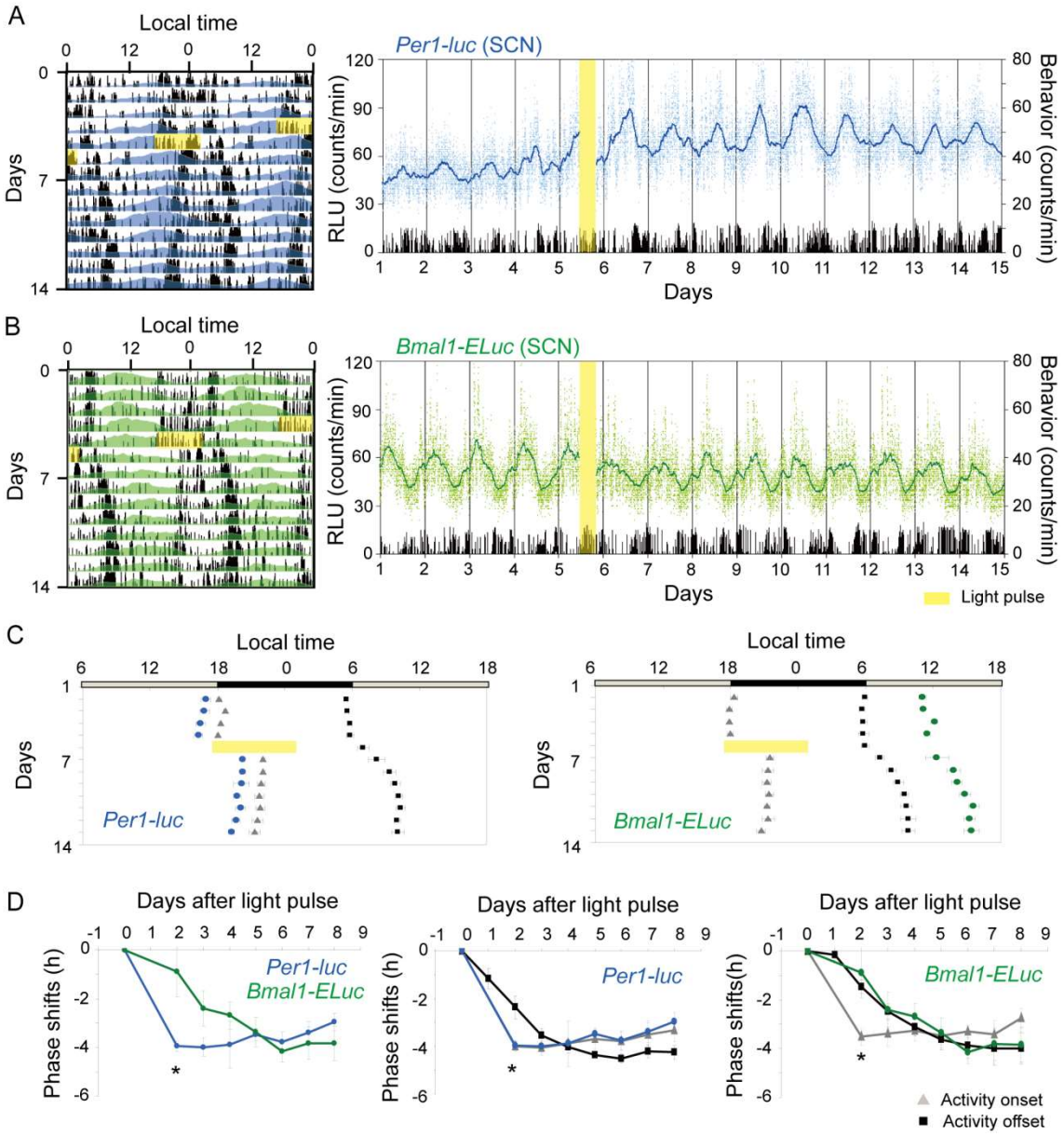

Figure 1: Light-pulse induced phase-delay shifts of circadian rhythms in the SCN and behavior rhythm in freely moving adult mice

Typical examples of phase-response at CT11.5 are illustrated for the circadian *Per1-luc* (A) and *Bmal1-ELuc* (B) rhythm with a behavior rhythm (black histogram) in double-plotting (left) where the colored area indicate bioluminescence larger than the minimum value of a series and in sequential plotting (right) where broken lines indicate raw data and solid lines 4 h

moving-averaged values (*Per1-luc*, blue; *Bmal1-ELuc*, green). The number of behavior activity was indicated at 1 min intervals with a black vertical bar. A yellow vertical bar indicates a time of light pulse. (C) Mean acrophases with SEM (horizontal bar) are illustrated for *Per1-luc* (blue circles, left) and *Bmal1-ELuc* (green circles, right) together with the mean activity onsets (gray triangles) and offsets (black squares). A yellow horizontal bar indicates a time of light pulse. A horizontal gray and black bar at the top of each panel indicates the LD cycle to which mice had entrained. (D) Daily phase-shifts are illustrated by the mean and SEM (n = 4) for *Per1-luc* (blue circle) and *Bmal1-ELuc* (green circle) (left), for *Per1-luc* and two phase markers of behavior rhythm (middle), and for *Bmal1-ELuc* and the phase-markers (right). The abscissa indicates days after a light pulse. An asterisk (*) indicates statistically significant difference ($P < 0.05$, two-way ANOVA with a post-hoc t-test) between *Per1-luc* and *Bmal1-ELuc* (left), between *Per1-luc* and activity offset (middle), and between *Bmal1-ELuc* and activity onset.

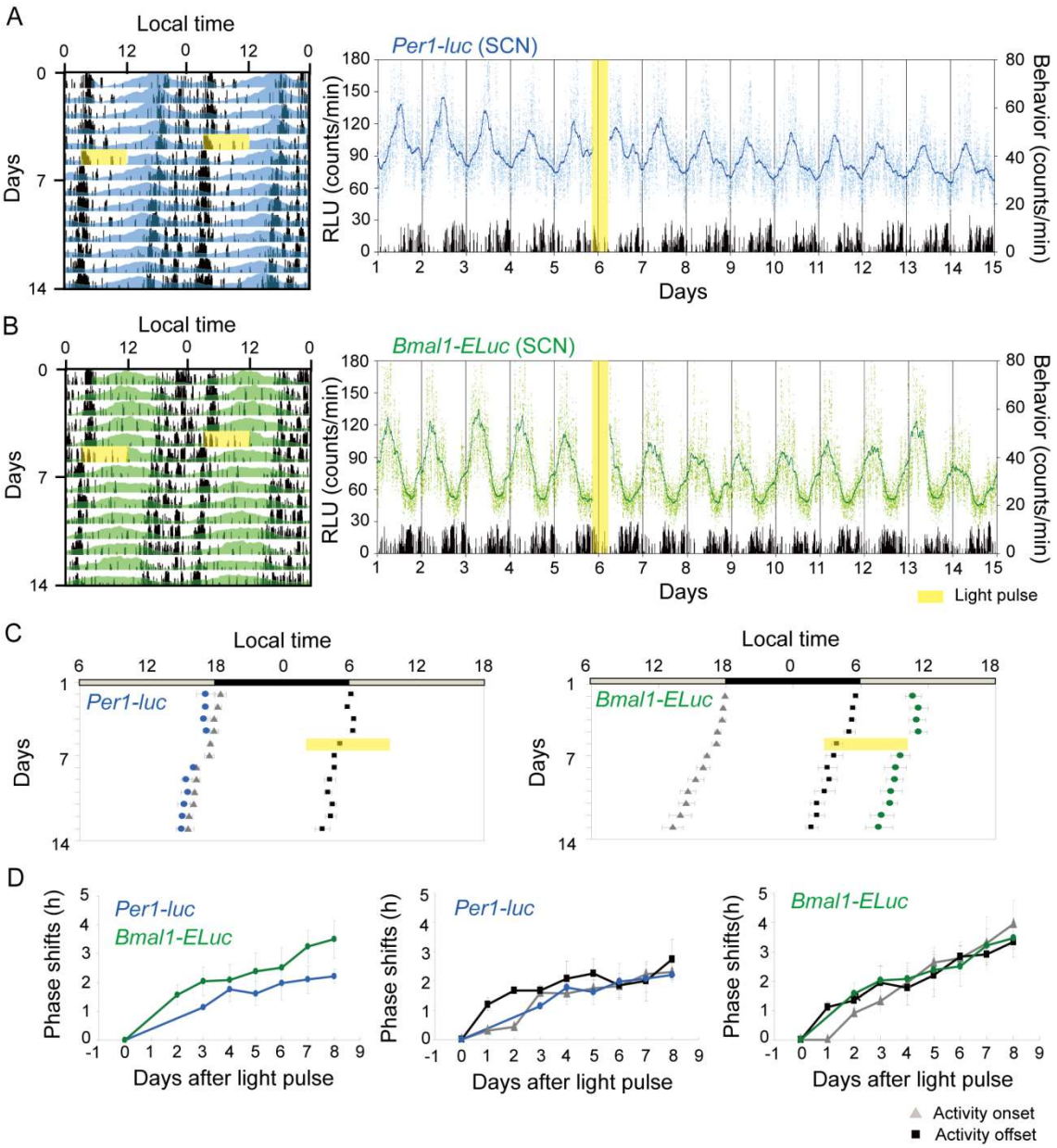

Figure 2: Light-pulse induced phase-advance shifts of circadian rhythms in the SCN and behavior rhythm in freely moving adult mice

Typical examples of a light-induced phase-response at CT21.5 are illustrated for the circadian *Per1-luc* (A) and *Bmal1-ELuc* (B) rhythm in the SCN with a behavior rhythm. The circadian rhythms are illustrated both in a double-plotted manner (left) and in sequential plotting (right). See also the legends for Figure 1A and B. (C) Mean acrophases are illustrated for *Per1-luc* (left) and *Bmal1-ELuc* (right) together with the mean activity onsets and offsets of

behavioral rhythms. See also the legend for Figure 1C. (D) The amount of phase-shifts after a light pulse are illustrated by the mean and SEM (n = 3) for *Per1-luc* (blue circles) and *Bmal1-ELuc* (green circles) (left), for *Per1-luc* and two phase markers (activity onset and offset) of behavior rhythm (middle), and for *Bmal1-ELuc* and the phase-markers (right). See also the legend for Figure 1D.

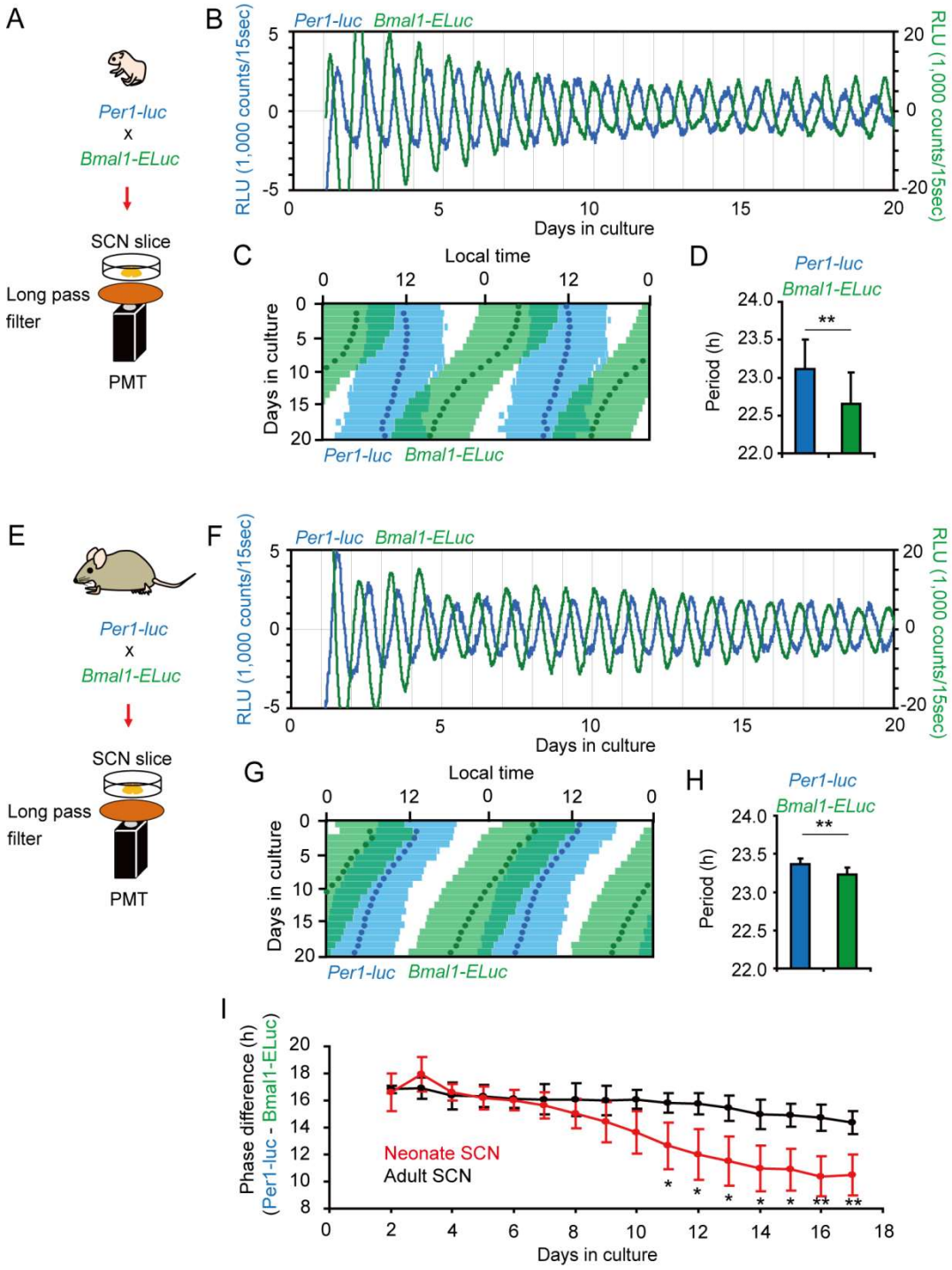

Figure 3: Simultaneous measurement of *Per1-luc* and *Bmal1-ELuc* rhythms in the cultured SCN slice

Experimental schemes of simultaneous measurement of *Per1-luc* and *Bmal1-ELuc* expressions in the neonatal (A) and adult (E) SCN slice. Sequential plots as well as double plots of circadian *Per1-luc* (blue) and *Bmal1-ELuc*

(green) rhythms of a neonatal (B, C) and an adult (F, G) SCN slice in culture. In double-plotting, the time zone where bioluminescence is higher than the mean value of detrended data in a series is indicated with color horizontal bars. Color circles in a double plot (C, G) are acrophases. Mean circadian periods calculated by χ square periodogram and SD (21 days) of *Per1-luc* and *Bmal1-ELuc* in the neonatal (n = 9) (D) and adult (n = 5) (H) SCN slices were indicated with colored columns. Asterisks (**) indicate statistically significant difference between *Per1-luc* and *Bmal1-ELuc* ($P < 0.01$, pared t-test). (I) Mean daily phase-differences in terms of acrophase between circadian *Per1-luc* and *Bmal1-ELuc* rhythms in the neonatal (red, n = 9) or adult (black, n = 5) SCN slices in culture for 17 days. Two-way repeated measure ANOVA revealed significant difference between the neonatal and adult SCN ($P < 0.01$). **: $P < 0.01$, *: $P < 0.05$, vs. adult SCN (post-hoc t-test).

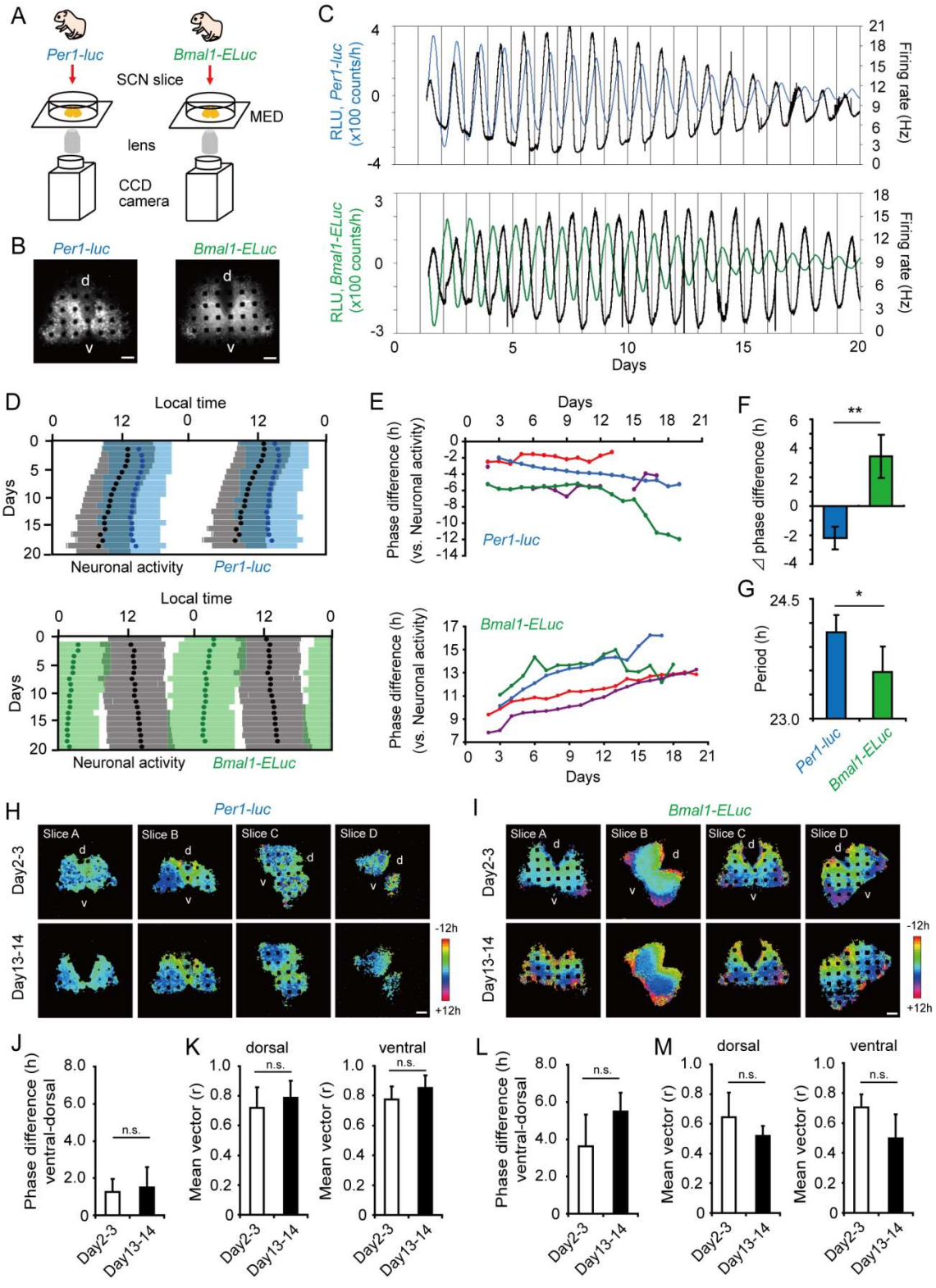

Figure 4: Simultaneous measurement of *Per1-luc* and *Bmal1-ELuc* together with spontaneous firing in the cultured SCN

(A) Experimental scheme of simultaneous measurement of *Per1-luc*, *Bmal1-ELuc* and spontaneous firing in the neonatal SCN. (B) Bioluminescence images of *Per1-luc* (left) and *Bmal1-ELuc* (right) on a MED probe. Scale bars are 100 μm. (C) Sequential plots of circadian *Per1-luc* (upper, blue) and *Bmal1-ELuc* (lower, green) with firing rhythm (black) from the entire area of the SCN. (D) Double plotted circadian rhythms of *Per1-luc* (upper, blue) and *Bmal1-ELuc* (lower, green) with respective acrophases (closed circles) are illustrated together with double plotted circadian rhythms of spontaneous firing (gray bars) with acrophase (black circles). The colored zones indicate the time where bioluminescence was higher than the mean value of detrended data in a series. See also the legend of Figure 3. (E) Daily phase, in terms of acrophase, differences of circadian *Per1-luc* (upper) or *Bmal1-ELuc* rhythm (lower) from firing rhythm in 4 SCNs with different colors. One SCN partially lacks firing data. (F) Phase difference (mean and SD) between Days 13-14 and 2-3 in culture for the circadian *Per1-luc* (left) or *Bmal1-ELuc* (right) rhythm. Negative values indicate phase-delay and positive phase-advance (**: $P < 0.01$, student's t-test). (G) Circadian period determined by χ square periodogram (mean and SD) using records of 14 days for *Per1-luc* and *Bmal1-ELuc* (*: $P < 0.05$, student's t-test). (H) Acrophase maps of *Per1-luc* and (I) *Bmal1-ELuc* at Days 2-3 (upper) and 13-14 in culture (lower) (n = 4). The mean acrophase was adjusted to 0 h. Color key indicates phase distribution in hours. The phase-difference (mean and SD) of circadian *Per1* (J) or *Bmal1* (L) rhythms on pixel level between the ventral and dorsal regions and the length of mean vector of respective rhythm (K, M) in the dorsal and ventral region are shown at Days 2-3 and 13-14 in culture.

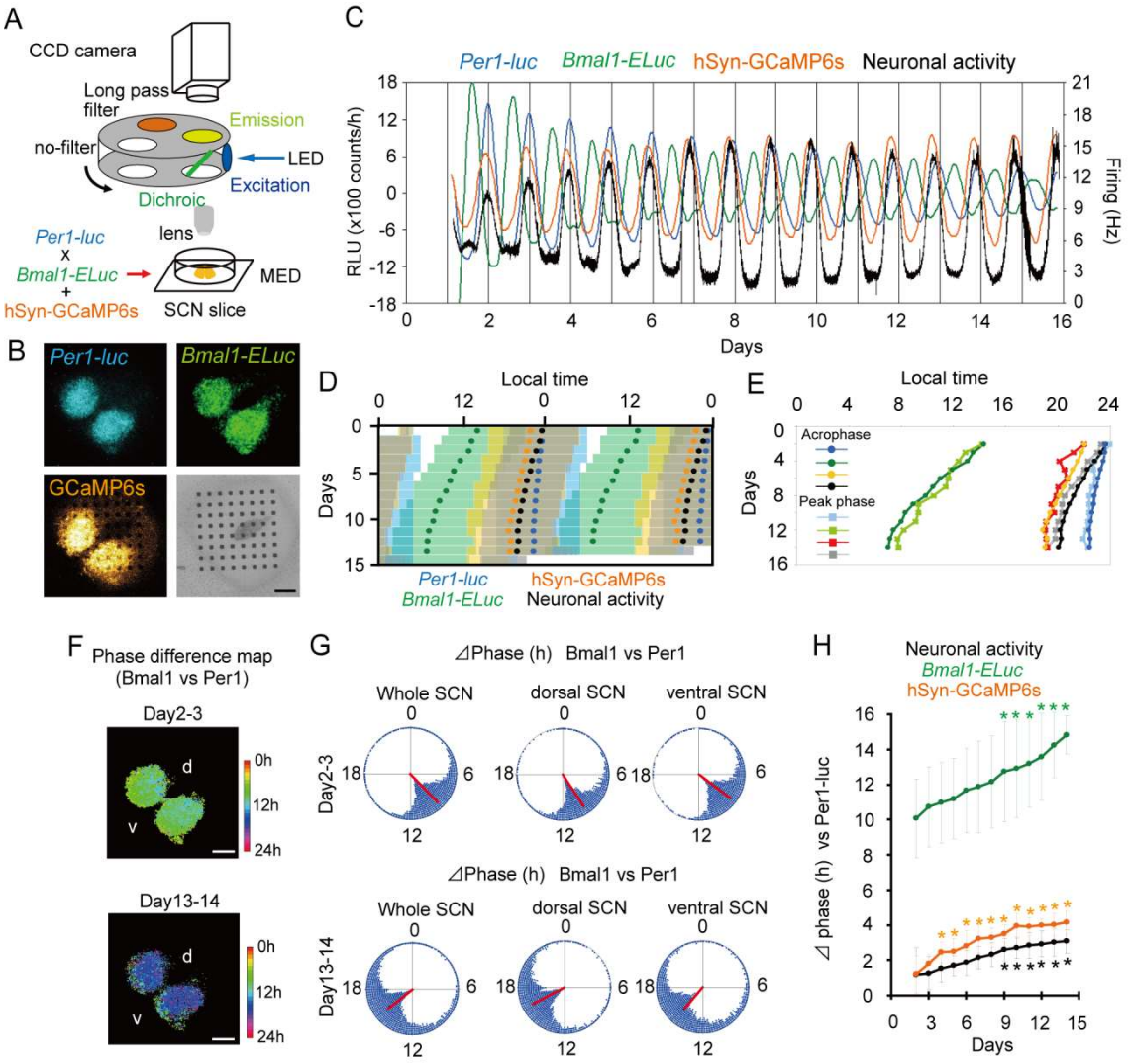

Figure 5: Simultaneous measurement of *Per1-luc*, *Bmal1-ELuc*, *intracellular calcium*, and *spontaneous* firing in the cultured SCN slice

(A) Experimental scheme of simultaneous multifunctional measurement in the neonate SCN slice. (B) Bioluminescence images of *Per1-luc* (upper left), *Bmal1-ELuc* (upper right), fluorescence image of GCaMP6s (lower left), and bright field image (lower right) of a cultured SCN slice on a MED probe. Scale bars are 200μm. (C) Sequential plots of circadian *Per1-luc*, *Bmal1-ELuc*, GCaMP6s, and firing rhythms from the entire area of the SCN. Spontaneous firing was expressed as the mean firing rate from electrodes covered by bilateral SCN. (D) Double plots of circadian rhythms of 4 measures. Colored circles are acrophases of circadian *Per1-luc*, *Bmal1-ELuc*, GCaMP6s, and firing rhythms. Yellow bars are the time zone where GCaMP6s fluorescence is higher than the

mean value of detrended data in a series. See also the legend of Figure 4D. (E) Longitudinal plotting of daily acrophases and of cycle peaks of four circadian rhythms demonstrated in Fig.5C. The features of free-running are almost identical regardless of the phase-marker. (F) Phase difference maps (*Per1-luc* vs. *Bmal1-ELuc*) at Day 2-3 (upper) and 13-14 in culture (lower). A color key indicates phase-difference in hours. (G) Rayleigh plots of phase difference on pixel level between *Per1-luc* and *Bmal1-ELuc* in the whole (left), dorsal (middle), and ventral (right) SCN are shown for Day 2-3 (upper) and 13-14 (lower) in culture. An arrow in a Rayleigh circle indicates the mean phase. (H) The mean daily phase-difference, in terms of acrophase, between the *Per1-luc* and other three circadian rhythms (n = 3). (*: $P < 0.05$, vs. Day 2, one-way repeated measure ANOVA with post-hoc Tukey-Kramer test).